PROCEEDINGS OF SCIENCE

Cosmic Ray Carbon and Oxygen Flux Measurements with the DAMPE Experiment

Yifeng Wei ,[a,b,*] Chuan Yue,[c] Dimitrios Kyratzis,[d,e,†] Felicia Barbato[d,e] and Mikhail Stolpovskiy[f] for the DAMPE Collaboration

[a] *State Key Laboratory of Particle Detection and Electronics, University of Science and Technology of China, Hefei 230026, China*

[b] *Department of Modern Physics, University of Science and Technology of China, Hefei 230026, China*

[c] *Key Laboratory of Dark Matter and Space Astronomy, Purple Mountain Observatory, Chinese Academy of Sciences, Nanjing 210023, China*

[d] *Gran Sasso Science Institute (GSSI), I-67100 L'Aquila, Italy*

[e] *Istituto Nazionale di Fisica Nucleare (INFN) - Laboratori Nazionali del Gran Sasso, I-67100 Assergi, L'Aquila, Italy*

[f] *Department of Nuclear and Particle Physics, University of Geneva, CH-1211 Geneva, Switzerland*

E-mail: weiyf@ustc.edu.cn, yuechuan@pmo.ac.cn, dimitrios.kyratzis@gssi.it, felicia.barbato@gssi.it, Mikhail.Stolpovskiy@unige.ch

The DArk Matter Particle Explorer (DAMPE), a space-based high-energy particle detector, has been operated in orbit for more than seven years. Thanks to its large geometric factor, good charge resolution and wide dynamic range in energy measurements, DAMPE can provide valuable insights into the energy spectra of cosmic ray carbon and oxygen up to tens of TeV/n. These measurements are fundamental for a better understanding of the origin, acceleration mechanism and propagation of cosmic rays in the Galaxy. In this paper, we present the latest progress in measurements of cosmic ray carbon and oxygen fluxes with the DAMPE experiment.

38th International Cosmic Ray Conference (ICRC2023)
26 July - 3 August, 2023
Nagoya, Japan

*Speaker

†Now at: Department of Nuclear and Particle Physics, University of Geneva, CH-1211 Geneva, Switzerland

PoS(ICRC2023)165

1. Introduction

Galactic Cosmic Rays (GCRs) are energetic particles traveling across the Galaxy, and are a unique probe to explore the astrophysical particle accelerators and the Interstellar Medium (ISM) of the Galaxy [1]. The energy spectrum of GCRs is expected to follow a power-law form for energies below the “knee” (at 3–4 PeV) according to the canonical shock acceleration of particles. However, several experiments have surprisingly observed changes in the power-law spectral indices γ for protons, helium, and heavy nuclei [2–10]. The deviations from a single power law of the spectra motivate extensive investigations for a deeper understanding of the acceleration and propagation mechanisms or of new possible GCR sources.

DAMPE is a general-purpose, satellite-based high-energy particle detector [11]. It was launched into a sun-synchronous orbit around the Earth at an altitude of 500 km on December 17, 2015. The scientific objectives of DAMPE are the search for dark matter decay or annihilation signatures, gamma-ray astronomy and the measurement of GCR fluxes. Thanks to its good performance and large acceptance, DAMPE has collected more than 13 billion events in seven years. It is expected to extend the measurement of cosmic ray carbon and oxygen up to tens of TeV/n. In this paper, we present latest progress in flux measurements of these two types of nuclei.

2. DAMPE detector

The DAMPE detector [11] is composed of the following sub-detectors (see Fig. 1): a Plastic Scintillator Detector (PSD) [12], a Silicon-Tugsten tracKer (STK) [13], a BGO imaging calorimeter [14], and a NeUtron Detector (NUD) [15]. The PSD is designed to measure the charge of incident particles up to Z =26 and provides an anti-coincidence veto signal for gamma rays. The STK is dedicated to precisely reconstruct the trajectories and measure the charge. The BGO calorimeter, which has a depth of 32 radiation lengths and 1.6 nuclear lengths, is responsible for the energy measurement and provides a powerful electron-proton discrimination. The NUD mainly improves the electron-proton separation power, especially for energies above TeV.

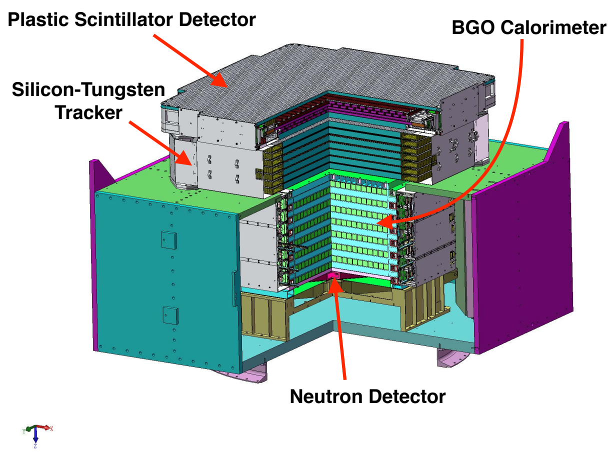

Figure 1: Schematic of the DAMPE instrument.

3. Data analysis

In this analysis, we used 84 months of the flight data recorded by DAMPE from January 1^{st}, 2016 to December 31^{st}, 2022. The number of collected events per day is about 5 million, and the data taking mode of DAMPE is very stable. After excluding the instrument dead time, the time for the on-orbit calibration, the time in the South Atlantic Anomaly (SAA) region, and the period between September 9, 2017 and September 13, 2017 during which a large solar flare affected the status of the detector [16], the total live time is 1.68×10^8 s, corresponding to 76.10% of the total operating time.

The results presented in this work are based on the GEANT4 toolkit of version 4.10.5 [17] with the FTFP_BERT physics list for nuclei between 10 GeV and 500 TeV. For the higher energies, we have adopted the EPOS_LHC model by linking the GEANT4 toolkit with the Cosmic Ray Monte Carlo (CRMC) interface [18].

3.1 Event selection

The data were further filtered with the following steps.

- Pre-selection
  First, the events were selected that passing the high energy trigger (HET). The HET requires that the energy deposition in the first three BGO layers be higher than about 13 times the proton minimum ionizing particle (MIP) energy (about 23 MeV in one layer) and in the fourth layer is higher than 2.4 times the proton MIP energy [19]. Then, the energy deposition in the calorimeter had to be greater than 60 GeV to avoid geomagnetic rigidity cutoff effects for carbon and oxygen. Finally, the energy recorded in each layer was required to be less than 35% of the total deposited energy. This requirement effectively excluded particles entering from the sides of the detector.

- Track Selection
  In general, the track-finding algorithm reconstructs multiple tracks in the STK, which are caused by CR pre-showering and backscattering effect of secondaries. Therefore, a number of criteria were set to derive the best track: a) the number of hits of the reconstructed tracks should be ≥ 3; (b) the angular difference between the STK tracks and the calorimeter reconstructed track should be less than 25 degrees; (c) the projected distances between the STK track and the centroids of the energy deposition in the first two BGO layers should be less than 30 mm; d) the reduced χ^2 of the track fit should be less than 25. In addition, to ensure good shower containment, the reconstructed track had to be fully contained in the PSD and BGO sub-detectors, and the bar with the maximum energy deposition in each layer had to be far away from the edge of the calorimeter.

- Charge selection
  Considering that protons and helium are the most abundant components in cosmic rays, a selection requiring the signal in the first STK layer to be greater than 500 ADC was applied in order to suppress such contributions. This criterion was very loose, since both carbon and oxygen signals were larger than 1000 ADC. The charge measurement with PSD was then

used to select carbon and oxygen candidates. The PSD charge reconstruction procedure included light attenuation (position) correction, light yield saturation (quenching) correction, and energy independence correction. A combined charge using multiple PSD sub-layers was employed to select carbon and oxygen candidates. Fig. 2 shows the combined PSD charge distribution for deposited energies of [359 - 464 GeV] and [2.0 - 3.4 TeV] in the BGO calorimeter, where the carbon and oxygen peaks can be clearly identified by eye. The selection windows $[Peak_C - 2FWHM_C, Peak_C + 2.5FWHM_C]$ and $[Peak_O - 2FWHM_O, Peak_O + 3FWHM_O]$ were used to obtain the carbon and oxygen candidates, respectively.

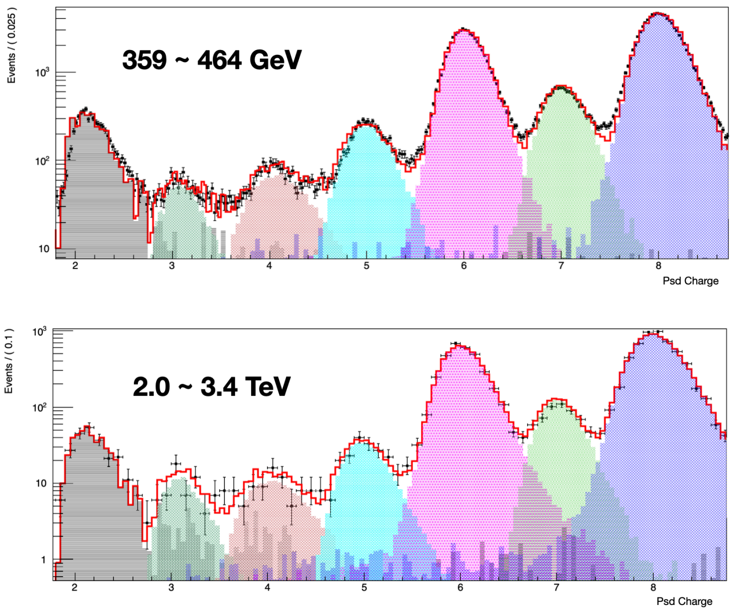

Figure 2: The combined PSD charge template fit for deposited energies in the range of [359 - 464 GeV] and [2.0 - 3.4 TeV] in the BGO calorimeter..

3.2 Background contamination

The backgrounds for carbon or oxygen included various misidentified nuclear species. The residual backgrounds were estimated using the best-fit MC nuclei templates with charge selection. The background contamination fractions from different nuclear species misidentified as carbon and oxygen are shown in Fig. 3. In the low energy range, the total contamination fractions are $\leq 1\%$ for both carbon and oxygen. Above 1 TeV, the shower backscattering from the calorimeter weakens the charge discrimination power, resulting in increase of contamination, especially from the abundant elements such as helium. Therefore, the contamination fractions increase up to $\sim 5\%$ and $\sim 3\%$ at 10 TeV for carbon and oxygen respectively.

3.3 Effective acceptance

The effective acceptance is defined as the product of the geometric factor and the selection efficiencies (including energy, trigger, track, and charge selections). The effective acceptance for

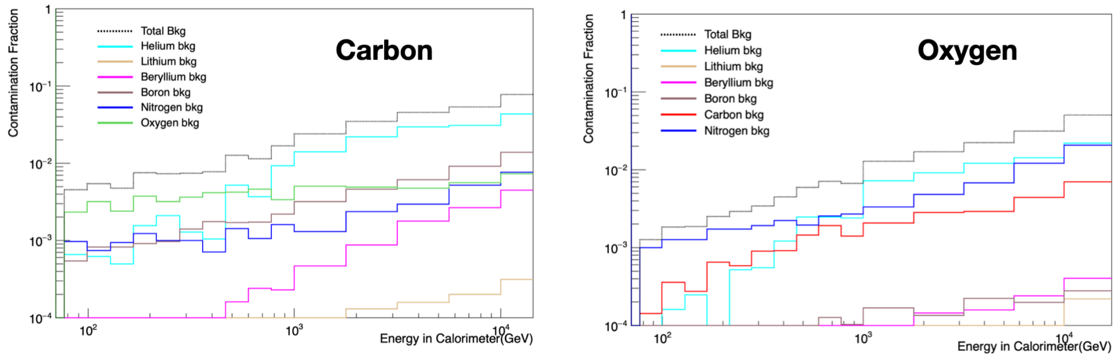

Figure 3: Carbon (left) and oxygen (right) contamination fractions.

the ith incident energy bin is calculated as

$$A_{eff,i} = A_{gen} \times \frac{N_{pass,i}}{N_{gen,i}} \tag{1}$$

where A_{gen} is the geometrical factor of the MC generation sphere and $N_{gen,i}$ and $N_{pass,i}$ are the numbers of generated events and those passing the selections, respectively. All efficiencies and the effective acceptance were obtained via the MC simulations. Fig. 4 shows the effective acceptance as a function of incident energy.

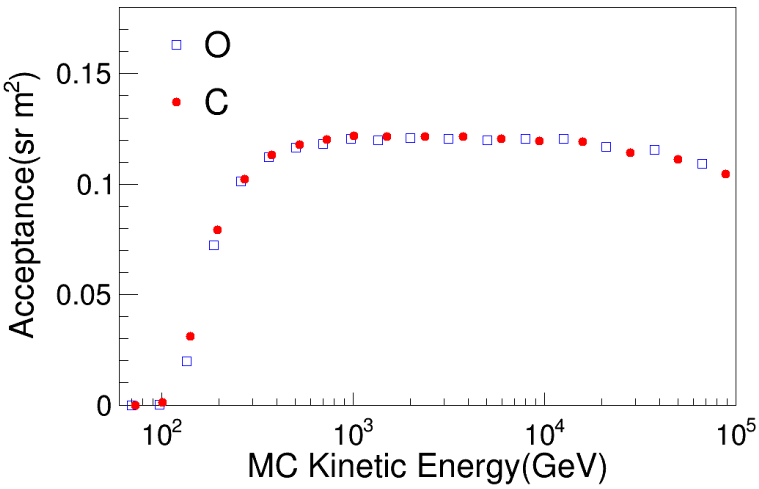

Figure 4: Effective acceptance for carbon (red dots) and oxygen (blue squares) after all analytical selects, as derived from the MC sample.

3.4 Energy unfolding

Due to the limited thickness of the BGO calorimeter ($\sim$ 1.6 nuclear length), a carbon or oxygen particle does not fully deposit its energy in the calorimeter. To convert the measured energy spectrum to the primary energy spectrum, it is necessary to unfold the instrument response. Rather than correcting the particle energy event by event, the unfolding procedure allows the energy distribution of the incident particles to be estimated from the deposit energy distribution. The number of events in the i-th deposited energy bin, $N_{dep,i}$, can be obtained from the sum of the number of events $N_{inc,j}$ in all the incident energy bins weighted by the energy response matrix. Equation 2 is solved using a Bayesian method to derive the incident event distribution. [20].

$$N_{dep,i} = \Sigma M_{ij} N_{inc,j} \tag{2}$$

where M_{ij}, the energy response matrix, is the probability that an event in the j-th incident energy bin is detected in the i-th deposited energy bin. The response matrix M_{ij} is derived from the GEANT4 FTFP_BERT simulations.

4. Summary

In this paper, we present the analysis procedure for carbon and oxygen flux measurements, including selection criteria, background estimation, and energy unfolding, etc. DAMPE has been operating smoothly for more than seven years. With further data accumulation, it is expected to measure carbon and oxygen fluxes up to tens of TeV/n with good precision. A more detailed analysis of the DAMPE data and a more precise estimation of the systematic uncertainties are ongoing.

5. Acknowledgement

The DAMPE mission is funded by the Strategic Priority Science and Technology Projects of CAS. In China the data analysis is supported by the National Key Research and Development Program of China (No. 2022YFF0503303), the National Natural Science Foundation of China (No. 12275266, No. 11673021, No. U1738205, No. U1738208, No. U1738139, No. U1738135, No. 11705197, No. 11851302), the strategic priority science and technology projects of Chinese Academy of Sciences (No. XDA15051100), the Youth Innovation Promotion Association CAS (Grant No. 2021450), the Outstanding Youth Science Foundation of NSFC (No. 12022503), the CAS Project for Young Scientists in Basic Research (No. YSBR-061). In Europe the activities and data analysis are supported by the Swiss National Science Foundation (SNSF), Switzerland, the National Institute for Nuclear Physics (INFN), Italy, and the European Research Council (ERC) under the European Union's Horizon 2020 research and innovation programme (No.851103).

References

[1] Grenier, Isabelle A., et al. Annu. Rev. Astron. Astrophys. 53 (2015): 199-246.

[2] Panov, A. D., et al. Bull. Russ. Acad. Sci. Phys. 73 (2009): 564-567.

[3] Ahn, H. S., et al. Astrophys. J. Lett. 714.1 (2010): L89.

[4] Adriani, Oscar, et al. Adv. Space Res. 51.2 (2013): 219-226.

[5] Aguilar, M., et al. Phys. Rep. 894 (2021): 1-116.

[6] DAMPE collaboration, et al. Sci. Adv. 5.9 (2019): eaax3793.

[7] Alemanno, F., et al. Phys. Rev. Lett. 126.20 (2021): 201102.

[8] Adriani, O., et al. Phys. Rev. Lett. 122.18 (2019): 181102.

[9] Adriani, O., et al. Phys. Rev. Lett. 125.25 (2020): 251102.

[10] Atkin, E., et al. J. Cosmo. Astropart. P. 2017.07 (2017): 020.

[11] Chang, Jin, et al. (DAMPE collaboration), Astropart. Phys. 95 (2017): 6-24.

[12] Yu, Yuhong, et al. Astropart. Phys. 94 (2017): 1-10.

[13] Azzarello, Philipp, et al. Nucl. Instrum. Methods Phys. Res., Sect. A 831 (2016): 378-384.

[14] Zhang, Zhiyong, et al. Nucl. Instrum. Methods Phys. Res., Sect. A 836 (2016): 98-104.

[15] Huang, Yong-Yi, et al. Res. Astron. Astrophys. 20.9 (2020): 153.

[16] https://solarflare.njit.edu/datasources.html.

[17] Agostinelli, Sea, et al. Nucl. Instrum. Methods Phys. Res., Sect. A 506.3 (2003): 250-303.

[18] Tykhonov, Andrii, et al. PoS 358 (2019): 143.

[19] Zhang, Yong-Qiang, et al. Res. Astron. Astrophys. 19.9 (2019): 123.

[20] D'Agostini, Giulio. Nucl. Instrum. Methods Phys. Res., Sect. A 362.2-3 (1995): 487-498.

PoS(ICRC2023)165